Elucidating the Native Architecture of the YidC

Kedrov, Alexej; Sustarsic, Marko; de Keyzer, Jeanine; Caumanns, Joseph J.; Wu, Zht Cheng; Driessen, Arnold J. M.

Published in:
Journal of Molecular Biology

DOI:
10.1016/j.jmb.2013.07.042

Publication date:
2013

Featured Article

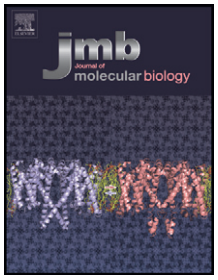

Elucidating the Native Architecture of the YidC: Ribosome Complex

Alexej Kedrov, Marko Sustarsic, Jeanine de Keyzer, Joseph J. Caumanns, Zht Cheng Wu and Arnold J.M. Driessen

Department of Molecular Microbiology, *Groningen Biomolecular Sciences and Biotechnology Institute, and Zernike Institute for Advanced Materials, University of Groningen, 9747 AG Groningen, The Netherlands*

Correspondence to Alexej Kedrov and Arnold J.M. Driessen: *A. Kedrov is to be contacted at: Gene Center Munich, Ludwig Maximilian University, Feodor-Lynen-Strasse 25, 81377 Munich, Germany, fax: +49 89 2180 76945; A. J. M. Driessen, University of Groningen, Nijenborgh 7, 9747 AG Groningen, The Netherlands Kedrov@genzentrum.lmu.de; A.J.M.Driessen@rug.nl.*
http://dx.doi.org/10.1016/j.jmb.2013.07.042
Edited by E. Nogales

Alexej Kedrov, Marko Sustarsic, Jeanine de Keyzer and Arnold J.M. Driessen

Abstract

Membrane protein biogenesis in bacteria occurs via dedicated molecular systems SecYEG and YidC that function independently and in cooperation. YidC belongs to the universally conserved Oxa1/Alb3/YidC family of membrane insertases and is believed to associate with translating ribosomes at the membrane surface. Here, we have examined the architecture of the YidC:ribosome complex formed upon YidC-mediated membrane protein insertion. Fluorescence correlation spectroscopy was employed to investigate the complex assembly under physiological conditions. A slightly acidic environment stimulates binding of detergent-solubilized YidC to ribosomes due to electrostatic interactions, while YidC acquires specificity for translating ribosomes at pH-neutral conditions. The nanodisc reconstitution of the YidC to embed it into a native phospholipid membrane environment strongly enhances the YidC:ribosome complex formation. A single copy of YidC suffices for the binding of translating ribosome both in detergent and at the lipid membrane interface, thus being the minimal functional unit. Data reveal molecular details on the insertase functioning and interactions and suggest a new structural model for the YidC:ribosome complex.

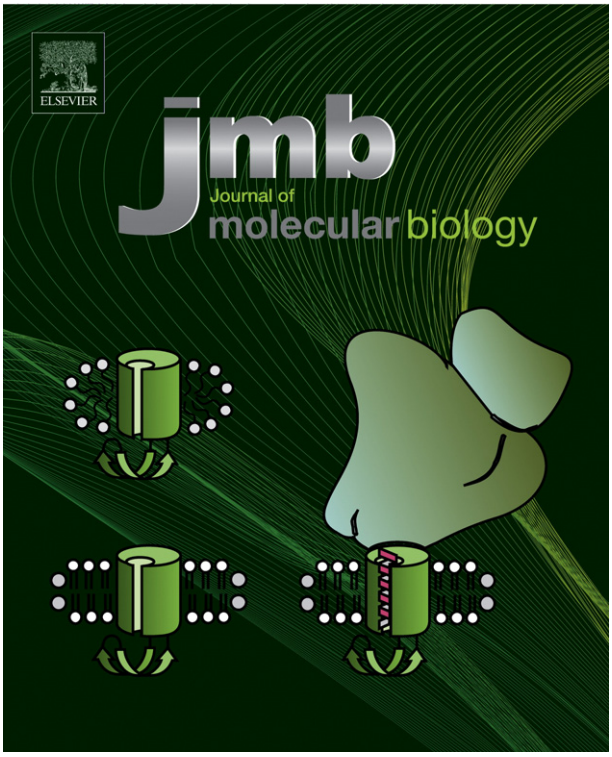

Legend: *Monomeric nanodisc-reconstituted insertase YidC interacts with ribosome-nascent chains of inner membrane proteins.*

Introduction

Understanding membrane protein folding, a key molecular process, remains one of the outstanding challenges in structural biology [1]. Membrane protein biogenesis occurs via evolutionarily conserved cellular systems, so-called insertases. These enzymes ensure the transfer of the newly synthesized polypeptide chain from the ribosome to the lipid bilayer, the correct integration of transmembrane domains, and their spatial packing to yield a functional membrane protein [2,3]. The model prokaryote *Escherichia coli* possess two membrane protein insertases, SecYEG and YidC. While the molecular mechanisms of SecYEG and its homologues have been explored to a large extent, there is only limited understanding on how YidC integrates proteins into the membrane [4]. YidC belongs to a universally conserved family of membrane protein insertases and is homologous to the Oxa1 protein of the mitochondrial inner membrane of eukaryotes and Alb3 of the thylakoid membrane in plant chloroplasts. It is generally anticipated that YidC and its counterparts in higher organisms are involved in the insertion and assembly of small membrane proteins. For instance, YidC facilitates the membrane insertion of the F_0c subunit of F_1F_0 ATP synthase [5] and the coat proteins of phages such as M13 and pf3 [6–8], and a broader specificity to multi-spanning membrane proteins has been suggested [9]. Apart from serving as an independent insertase, YidC facilitates membrane protein integration via a functional cooperation with the SecYEG complex [10,11]. YidC has also been implicated in membrane protein folding and assembly into multisubunit membrane protein complexes [12,13]. A detailed mechanism of the YidC activity at the membrane interface remains unknown in spite of extensive efforts in molecular analysis [3].

Due to the low structural conservation among the members of the YidC/Oxa1/Alb3 family and its high tolerance to mutations, YidC may serve as a platform for membrane protein integration, possibly in complex with the ribosomes [14]. A cross-linking study on YidC within native membranes suggested that YidC interacts with both empty and translating ribosomes, while the interaction sites appear not to be limited to the ribosomal tunnel region but distributed over the large and small ribosomal subunits [15]. The exact functional implications of this large contact area are unclear. Recently, binding of detergent-solubilized YidC to translating ribosomes was visualized by single-particle electron microscopy, and a dominant role in the complex formation was assigned to a short C-terminal region of YidC [16]. Based on low-resolution data, two copies of YidC were implied to bind the ribosome at the ribosomal tunnel exit (L23 and L28 proteins) possibly forming a consolidated pore for the emerging substrate. While the model matched previous two-dimensional crystallographic data on the YidC apo-form in a membrane environment [17] and biochemical analysis [18], its physiological relevance is unknown.

Available information on YidC structure remains limited and only describes selected states of the protein upon its functional cycle. Although even low-resolution snapshots of membrane proteins often give new insights into their spatial organization and key interaction forces, the physiological interactions may be disrupted due to introduced factors, such as detergent, unnatural buffer conditions, and the use of recombinant proteins equipped with tags, and these may mislead the structure interpretation [19]. This poses the need for complementary studies in native membrane conditions. Here, we investigated the molecular forces that drive the YidC:ribosome interaction in both detergent-solubilized and membrane-embedded states. We implemented fluorescence correlation spectroscopy (FCS) and fluorescence cross-correlation spectroscopy (FCCS) to analyze isolated YidC molecules present in detergent micelles and lipid membranes within nanodiscs and quantify their ability to bind ribosomes. Our data demonstrate that the molecular environment determines to a large extent the properties of YidC to interact with ribosomes in their different translation states, while the lipid bilayer determines the specificity of YidC to translating ribosomes. We confirm on the molecular level that the C-terminal domain of YidC is involved but that it is not essential for ribosome recruitment. Most importantly, we show that a single membrane-embedded YidC copy is sufficient to bind a substrate-translating ribosome, thus being a minimal functional unit.

Results

YidC:ribosome interaction in detergent solution

To monitor the interaction of YidC with ribosomes, we aimed to employ high-sensitivity fluorescence detection methods. A hexa-histidine tag was conjugated to the YidC C-terminal end for purification needs. A single cysteine was introduced at the non-conserved position 269 within the P1 domain [20] of cysteine-less YidC allowing conjugation of a fluorescent marker followed by YidC purification (Fig. 1a–c). Fluorescently labeled YidC was reconstituted into proteoliposomes formed of a synthetic lipid mixture [1,2-dioleoyl-*sn*-glycero-3-phospho-(1′-rac-glycerol):1,2-dioleoyl-*sn*-glycero-3-phosphoethanolamine:1,2-dioleoyl-*sn*-glycero-3-phosphocholine, 3:3:4 molar ratio] that was previously shown to form stable proteoliposomes and that fully supports protein translocation activity by SecYEG [21]. To probe for the YidC activity, we analyzed the membrane integration of a natural substrate, the F_0c subunit of the F_1F_0 ATP synthase, into proteoliposomes using a protease protection assay [22]. In the

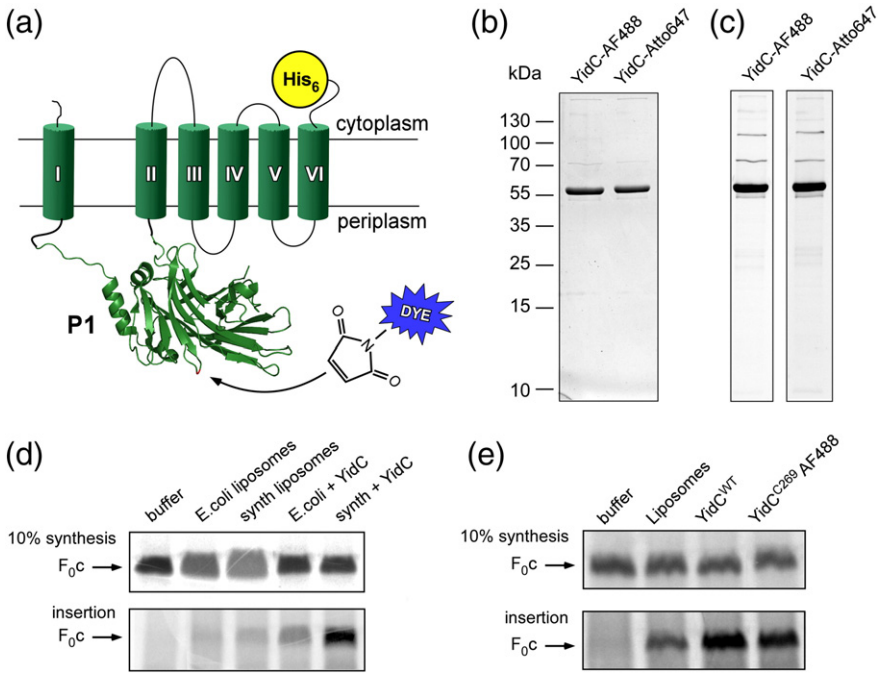

Fig. 1. Reconstitution of the YidC insertase activity *in vitro*. (a) Structural model of YidC. Recombinant YidC contained a C-terminal hexa-histidine tag and a unique cysteine at position 269 (marked red) within the periplasmic domain P1. Maleimide derivatives of fluorophores AlexaFluor 488 and Atto 647N were conjugated to YidC at this defined position, and the protein was purified for further analysis. (b) Coomassie-stained SDS-PAGE of labeled and purified YidC, with a molecular mass of 62 kDa. Molecular masses of protein markers are indicated on the left. (c) YidC-conjugated fluorophores were visualized within the SDS-PAGE prior to Coomassie staining. (d) Synthetic lipids support YidC activity. ^{35}S-Labeled F_0c subunit of ATP synthase was incorporated into YidC-containing proteoliposomes composed of either *E. coli* polar lipid extract ("E.coli") or synthetic lipid composition ("synth"). Liposomes without YidC ("liposomes") were used to probe for spontaneous insertion of F_0c. (e) Mutations and fluorophore conjugation does not affect the YidC activity. Proteoliposomes were composed of synthetic lipids and contained identical levels of wild-type YidC ("YidC^{WT}") and single-cysteine mutant of YidC conjugated to AlexaFluor 488 dye ("YidC^{C269AF488}").

presence of YidC, the synthetic liposomes supported high levels of membrane-inserted F_0c (Fig. 1d), showing that YidC retained its activity upon the introduction of mutations and fluorescent labeling (Fig. 1e).

To monitor the YidC:ribosome complex assembly, we used FCS. FCS allows the characterization of the diffusion of fluorescently labeled molecules present at nanomolar concentrations, wherein the measured diffusion coefficient is inversely proportional to the hydrodynamic radius of the molecule (Fig. 2a) [23]. The YidC-AlexaFluor 488 diffusion was analyzed in a slightly acidic environment (pH 6.2) to match closely the conditions reported by Kohler *et al.* in the cryo-electron microscopy (cryo-EM) study (pH 5.8) [16]. FCS recordings resulted in a typical sigmoidal auto-correlation trace (Fig. 2b), and the rapid decay in the correlation signal could be attributed to YidC diffusion through the confocal volume. For YidC in its *n*-dodecyl β-D-maltoside (DDM)-solubilized state, the average focal residence time of approximately 200 μs corresponded to a diffusion coefficient *D* of 42 ± 1 cm^2/s. Previously, we observed that DDM-solubilized SecYEG has a 1.5-fold lower mobility [24] even though its molecular mass is similar to that of YidC, 70 and 67 kDa, respectively. The difference in the diffusion likely emerges from differences in shapes, number of transmembrane domains, and size of detergent micelles surrounding the proteins that determine their hydrodynamic radii [25].

Binding of YidC-AlexaFluor 488 to ribosomes should decrease its diffusion rate due to the much larger molecular radius of the formed complex (Fig. 2a) [24]. Indeed, when purified ribosome:nascent chain (RNC) complexes that expose the N-terminal transmembrane segment of F_0c (RNC-F_0c; Fig. S1) were added in 5- to 10-fold excess (400–500 nM), a substantial shift in the YidC auto-correlation traces toward longer residence times (700–800 μs) was observed (Fig. 2b). To quantify the binding efficiency of YidC to the RNC, we fitted the auto-correlation traces with a two-component model as described previously [24] and assuming the presence of both free and RNC-bound YidC in solution. The population of each component was determined from the fit. About 80% of the YidC molecules were bound to RNC at the assayed acidic conditions (Fig. 2c). We also analyzed

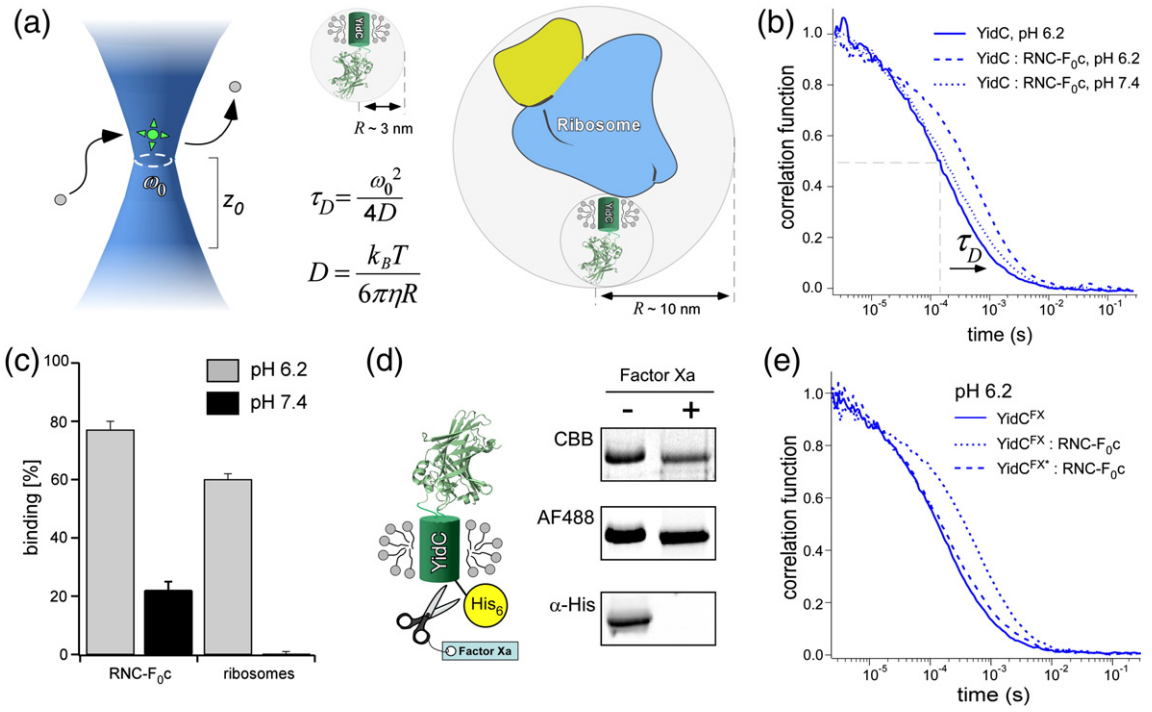

Fig. 2. YidC:ribosome interactions in the detergent environment. (a) YidC diffusion analysis by FCS. Fluorophore-conjugated YidC molecules diffused through the illuminated confocal volume with the lateral size ω_0 and the vertical size z_0. Average residence time within the focal volume determined from the auto-correlation curve is in inverse proportion to the diffusion coefficient D of YidC that is determined by the hydrodynamic radius of the molecule. Size estimates for free and ribosome-bound YidC are shown. (b) FCS analysis on YidC:ribosome interactions. Normalized auto-correlation traces recorded on 50 nM YidC in its free state and in the presence of 300 nM RNC complexes (RNC-F_0c) at different pH are shown. The shift in the auto-correlation traces indicated changes in the diffusion coefficient of YidC upon the ribosome binding. (c) YidC:ribosome binding efficiency at different pH. FCS data revealed that ribosome binding was strongly enhanced under acidic conditions. Non-translating ribosomes ("ribosomes") showed lower YidC binding compared to RNC-F_0c. (d) Designing tag-less YidC variant. Hexa-histidine tag was removed from the YidC^{FX} construct by specific proteolysis. Removal of the tag caused shift of both CBB-stained and fluorescent YidC band on SDS-PAGE and was confirmed by Western blotting against the histidine tag. (e) Protonation of the histidine tag dictates YidC:ribosome interactions. Protease-processed YidC^{FX*} lacking the tag showed minor 22% RNC binding at the acidic conditions. Control tagged YidC^{FX} showed slow diffusion in the presence of RNC-F_0c and was competent for the ribosome binding.

the interaction of YidC with non-programmed ribosomes (Fig. S1). Again, we observed a decrease in the YidC mobility, though the binding efficiency was reduced to 60% (Fig. 2c).

Several independent studies suggest a role of the C-terminal end of YidC homologues in the interaction with ribosomes [26–28]. This cytoplasmic domain typically contains long stretches of positively charged amino acids, which are likely to assist in ribosome docking via electrostatic interactions. The C-terminal domain of *E. coli* YidC contains only 13 amino acids including 7 arginines and lysines [29] and, thus, is relatively short compared to the C-termini of YidC proteins for which ribosome binding has been firmly established. The recombinant YidC protein used for the cryo-EM studies [16,17] and replicated here is extended by a hexa-histidine tag that will be protonated at pH 6 and below. This increased positively charged character may facilitate ribosome binding in a non-physiological manner. To assess the specificity of the YidC:ribosome interaction, we investigated the binding reaction at an elevated pH 7.4 that corresponds to the physiological environment of the bacterial cytoplasm. Other components of the solution were not altered, including ADA as the buffering agent. Diffusion of YidC-AlexaFluor 488 alone occurred at similar rates as at pH 6.2 described above, $D = 43 \pm 3$ cm^{-2}/s. However, in contrast to the acidic conditions, the addition of RNC-F_0c at pH 7.4 only slightly affected the auto-correlation curve of YidC (Fig. 2b) suggesting that a large fraction of YidC remained in its free state. Indeed, two-component analysis of the FCS data revealed RNC binding of only 23% of YidC (Fig. 2c). Furthermore, the interaction was completely abolished if non-programmed ribosomes were used.

To validate a contribution of the histidine tag of the recombinant YidC in the interaction, we designed a variant of YidC with a cleavable histidine tag (YidC^{FX}) that allowed removing the tag with factor Xa protease (Fig. 2d). When using the tag-less YidC^{FX*} in the FCS

experiments, binding of RNC-F_0c at acidic conditions was reduced to only 22% (Fig. 2e). This binding was barely altered by an increase of the pH to the physiological value of pH 7.4, again showing complex formation with RNCs by 19% of the YidC. From these experiments, we conclude that the histidine tag strongly promotes the association of the recombinant and detergent-solubilized YidC with RNCs and empty ribosomes at acidic conditions that may not reflect naturally occurring interactions. Moreover, under physiological buffer conditions, YidC interacts only with translating ribosomes.

Oligomeric state of YidC in detergent solution

Early studies on YidC extracted from bacterial membranes suggested that the protein is present in both monomeric and dimeric forms [22,30].

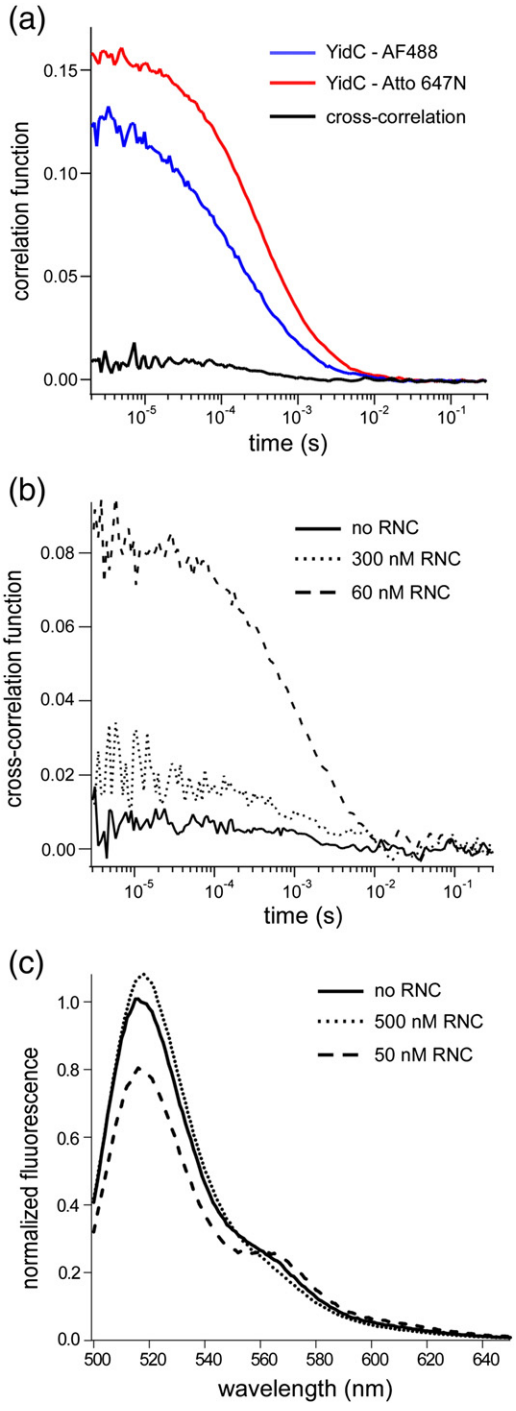

Fig. 3. Oligomeric state of detergent-solubilized YidC. (a) Purified YidC exists in monomeric form. YidC was incubated in the presence of spectrally separated fluorophores and was subject to FCCS analysis at pH 6.2. The amplitude of the cross-correlation signal did not exceed 10% and reflected limited unspecific labeling of YidC, that is, those molecules that bear both fluorophores, while no YidC oligomers could be detected. (b) YidC monomers are competent to bind ribosomes. Differentially labeled histidine-tagged YidC (50 nM) was incubated with varying concentrations of programmed RNCs at pH 6.2. In the presence of an excess RNCs (300 nM), no substantial YidC oligomerization was detected, as cross-correlation signal was nearly at background levels. At the YidC:RNC ratio approaching 1:1, strong cross-correlation was observed, suggesting several copies of YidC binding to a single ribosome. (c) Oligomerization of YidC is concentration dependent. YidC molecules labeled with AlexaFluor 488 and Cy3 fluorophores were analyzed for FRET in their free and RNC-bound states. No FRET signal was measured for freely diffusing YidC (100 nM) or bound to the excessive amounts of RNC (500 nM), while acceptor fluorescence, and thus YidC oligomerization, was detected upon adding low amounts of RNC (50 nM).

Crystallographic analysis suggested that YidC forms symmetric dimers in the membrane [17], while the cryo-EM study on the YidC:RNC-F_0c complex suggested that two copies of YidC bind to the ribosomal tunnel exit [16]. Also, weak cross-linking between detergent-solubilized YidC protomers was observed in the presence of RNCs. To probe the oligomeric state of YidC in its free form and bound at the ribosome, we implemented FCCS [31]. This technique measures the fluorescence intensities of spectrally separated fluorophores and correlates those over time, thus reporting on their co-migration or independent diffusion. For the FCCS experiment, YidC-containing membranes were solubilized and two spectrally different fluorophores, AlexaFluor 488 and Atto 647N, were added simultaneously; thus, labeling of individual YidC protomers with either of the dyes could occur stochastically. We achieved total YidC labeling of about 110% that consisted of 60% AlexaFluor 488 and 50% Atto 647N and a small contribution of unspecific labeling of about 5–10% for each fluorophore (Fig. S2). The FCCS analysis performed in 0.1% DDM at pH 6.2 confirmed that less than 10% of the YidC species contained both fluorophores matching the unspecific labeling level (Fig. 3a). Alternatively, AlexaFluor 488 and Atto 647N fluorophores were conjugated to YidC in individual reactions and the differently labeled YidC molecules were mixed together to probe the association of hetero-oligomers. Only weak cross-correlation signal was measured (below 5%), showing that YidC was present exclusively as monomers in detergent solution.

To assay YidC:RNC complex formation, we diluted the dual-labeled YidC in DDM to a concentration of 50 nM and mixed it with 300 nM RNC-F_0c at pH 6.2. A large shift in auto-correlation curves recorded for both YidC labeled with AlexaFluor 488 and Atto 647N occurred consistent with the YidC being bound to the RNCs. However, the cross-correlation signal was barely affected (Fig. 3b), suggesting that YidC largely remained in its monomeric state when bound to the ribosomes. The observation that a single YidC copy is sufficient for binding ribosomes opposes earlier results from the cryo-EM study [16]. However, we observed a substantial increase of the FCCS signal and, thus, YidC oligomerization when the RNC-F_0c concentration was reduced to 60 nM (Fig. 3b). The apparent diffusion time measured for YidC oligomers from the FCCS trace (~950 μs) matched well with the value recorded on the ribosomes alone [24], indicating that the YidC oligomerization indeed occurred on the ribosome. In a complementary experiment, YidC proteins were labeled with AlexaFluor 488 and Cy3 fluorophores, which form a pair for Förster resonance energy transfer (FRET). Differently labeled YidC proteins were mixed at equimolar ratio at final concentration of 100 nM, and the oligomeric state of YidC was probed via conventional FRET measurements. For freely diffusing YidC, the emission spectrum was dominated by AlexaFluor 488 (donor) fluorescence with a characteristic peak at 520 nm, and it was barely affected in the presence of 5-fold excessive amounts of RNC (Fig. 3c). However, when YidC and ribosomes were present at 2:1 molar ratio, a pronounced signal from the Cy3 fluorophore (acceptor) was detected at 570 nm, while the donor fluorescence was decreased, suggesting efficient FRET between two ribosome-bound YidC copies. Since a 10-fold excess of YidC was used previously to form YidC:RNC complexes [16], the corresponding cryo-EM structure likely resolved a concentration-dependent oligomer of YidC.

YidC:ribosome interaction in lipid membranes

Detergents often do not fulfill all requirements for membrane protein functioning due to a lack of specific polar/apolar interactions and/or altered lateral pressure profiles [19,32]. For instance, we have previously demonstrated a strong effect of the molecular environment on the binding properties of SecYEG to its ligands, that is, ribosomes and the SecA motor protein [24]. An alternative to the detergent-solubilized state is the reconstitution of membrane proteins into small lipid patches known as nanodiscs [33]. Nanodiscs of a pre-defined size are formed by two copies of a major scaffold protein (MSP) that build a boundary for 100–200 lipid molecules forming a bilayer. Depending on the length of the MSP construct, the enclosed bilayer area ranges between 40 and 90 nm^2. The bilayer area is typically sufficient to accommodate single or multiple integral membrane proteins, thus providing a physiologically relevant environment that supports protein activity [34].

YidC-AlexaFluor 488 was reconstituted into nanodiscs in 10-fold excess of the MSP to achieve a monomeric state of YidC in the nanodiscs (Fig. 4a). According to the Poisson distribution, 16% of formed nanodiscs were predicted to contain YidC monomers and the fraction of nanodiscs that contained multiple copies of YidC was predicted below 3%, leaving the remaining 80% nanodisc empty. These monomeric $YidC^{mono}$-Nd samples were subjected to size-exclusion chromatography to remove occasional aggregates or liposomes. $YidC^{mono}$-Nd repeatedly eluted at fractions #14 and #15, while nanodiscs containing pure lipids eluted at fraction #16 and later (Fig. 4b). The shift in the elution profile is likely to occur because of the large (30 kDa) periplasmic domain of YidC that is exposed above the membrane surface, thus contributing to the hydrodynamic radius of the $YidC^{mono}$-Nd assembly. Resulting discs were about 10 nm diameter as verified by the negative-stain electron microscopy, and the monomeric state of YidC was confirmed by FCCS using

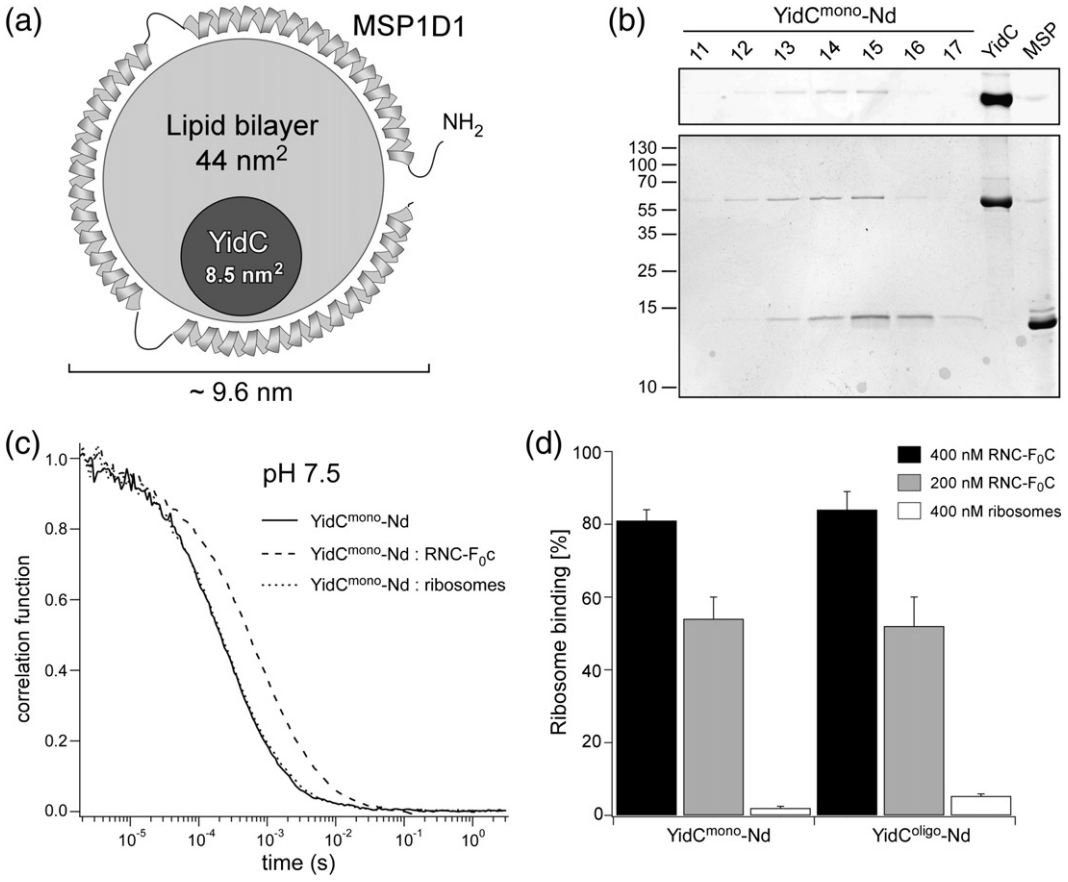

Fig. 4. Lipid-reconstituted YidC specifically interacts with RNCs. (a) Structural organization of a YidC-containing nanodisc (YidC-Nd). A single YidC copy occupies below 20% of the nanodisc inner surface area. (b) Isolation of YidC-Nd. YidC-Nd were fractionated and separated from empty nanodiscs upon size-exclusion chromatography as shown on SDS-PAGE (top, AlexaFluor 488 fluorescence; bottom, Coomassie staining). Fraction #14 was used for further analysis. (c) FCS analysis on YidC-Nd:ribosome interactions. Normalized auto-correlation curves recorded on YidC-Nd in the absence and presence of ribosomes and RNCs at pH 7.5 showing a shift upon RNC binding to YidC. (d) The oligomeric state of YidC does not affect the ribosome binding. FCS experiments on ribosome binding to nanodiscs containing single ($YidC^{mono}$-Nd) and multiple ($YidC^{oligo}$-Nd) copies of YidC did not reveal differences in the binding efficiency.

the YidC labeled with AlexaFluor 488 and Atto 647N as described in the previous section (Fig. S3). Diffusion of $YidC^{mono}$-Nd was characterized by FCS at pH 7.5 to avoid protonation of the histidine tag (Fig. 4c), and the diffusion coefficient of 31 ± 2 cm^2/s matched closely the value previously recorded for SecYEG nanodiscs [24]. In the following step, we added RNC-F_0c in 5-fold excess to $YidC^{mono}$-Nd and analyzed the binding efficiency based on the shift in $YidC^{mono}$-Nd auto-correlation traces. About 80% of $YidC^{mono}$-Nd formed complexes with the RNCs at pH 7.5, and RNC binding was concentration dependent (Fig. 4d), contrasting the detergent-solubilized YidC that binds RNCs with low affinity (Fig. 2c). However, when non-programmed ribosomes were added, no change in $YidC^{mono}$-Nd mobility was observed, demonstrating that YidC only interacts with RNCs that contain an emerging nascent chain. These result support previous observation on YidC:ribosome interactions within biological membranes and show for the first time that single YidC protomer is competent for interactions with ribosomes containing a nascent chain.

To study the properties of YidC oligomers, we reconstituted the insertase into nanodiscs at high YidC:MSP ratio that ensured multiple copies of YidC embedded within single nanodiscs ($YidC^{oligo}$-Nd). According to the Poisson distribution, reconstitution of YidC into nanodiscs at a 2:1 molar ratio would result in 27% nanodiscs containing one copy of YidC and about 60% nanodiscs containing multiple YidC molecules, with “dimers” as the most abundant species. Assuming that the orientation of YidC within a nanodisc is stochastically driven, physiologically oriented dimers will be present in about 35% of the formed nanodiscs, while this value will decay rapidly for higher oligomers approaching 1% for YidC tetramers. The presence of multiple copies of YidC per nanodisc within the $YidC^{oligo}$-Nd sample was

monitored by FCCS using YidC labeled with Alexa-Fluor 488 and Atto 647N (Fig. S3). Based on the cross-correlation analysis, we concluded that above 60% of the YidC^{oligo}-Nd contained multiple YidC molecules in the selected fraction. Auto-correlation traces showed similar, within 10% difference, diffusion times for YidC^{mono}-Nd and YidC^{oligo}-Nd samples that reflected similar dimensions of formed nanodiscs (Fig. S3). When adding empty or translating ribosomes to YidC^{oligo}-Nd, we found that YidC^{oligo}-Nd were able to bind RNC-F_0c, but not empty ribosomes. Importantly, binding occurred at similar level as for YidC^{mono}-Nd (Fig. 4d) suggesting that monomeric YidC is fully compatible for building a functional complex with ribosomes.

In vivo complementation studies showed that the deletion of the C-terminal domain (YidCΔC) has no effect on bacterial growth, showing that the domain is not essential for the activity [14]. In contrast, a co-sedimentation assay performed by Kohler *et al.* on the detergent-solubilized YidC showed that no interactions occurred between YidCΔC and 70S ribosomes [16]. However, no analysis on translating ribosomes was performed, and the experiments were conducted under acidic conditions that promote binding of the histidine-tagged YidC to ribosomes, as described above. Therefore, we further investigated functional properties of the C-terminal truncated YidC. The YidCΔC construct was analyzed for its ability to complement the YidC depletion strain FTL10 [35]. Both histidine-tagged and non-tagged YidCΔC fully rescued the growth defect of the deletion strain (Fig. 5a), in agreement with previous results [14]. Remarkably, liposome-reconstituted YidCΔC mutant also supported insertion of the model substrate F_0c at the same level, similar to wild-type YidC (Fig. 5b). As YidC^{mono}-Nd is competent for RNC binding, we purified and reconstituted monomers of YidCΔC into nanodiscs to assess the role of the C-terminal domain of YidC in the interaction. The YidC^{mono}ΔC-Nd was competent for RNC binding, though the efficiency substantially reduced from 80% to 21 ± 3% (Fig. 5c). These data show that the short C-terminal end of YidC is not essential for the interaction between YidC and translating ribosomes but enhances the affinity for complex formation.

Discussion

Here, we present a detailed analysis of the interaction between the conserved YidC insertase and ribosomes and demonstrate that the assembly of the YidC:ribosome complex depends on both properties of the interacting molecules and their environment. Employing lipid-containing nanodiscs rather than conventional proteoliposomes allowed us to design a system suitable for quantitative fluorescence spectroscopy and to analyze the assembly of the YidC:ribosome complex to define the quaternary structure of the insertase.

Extensive research performed on the eukaryotic YidC homologue Oxa1 validated its interactions with ribosomes upon substrate insertion [26,27]. Also, evidence for ribosome binding to purified detergent-solubilized YidC and YidC present in native membranes has been presented previously [15,16]. However, these studies yielded contradictory results, and thus, the specificity for YidC:ribosome complex formation, its molecular architecture, and the recognition mechanism have remained elusive. Recently, Kohler *et al.* described the low-resolution cryo-EM structures of both Oxa1 and YidC proteins, and it was suggested that they form symmetric dimers at the substrate exit of a translating ribosome. Remarkably, the YidC:ribosome complex was formed and visualized at non-native acidic conditions, below pH 6. These non-native conditions likely were necessary to efficiently produce stable YidC:ribosome complexes for cryo-EM investigation. Based on a robust fluorescence-based approach, we now show that the pH-dependent electrostatic interactions strongly stimulate YidC:ribosome complex formation in the detergent environment, caused by the use of a recombinant form of YidC with a hexa-histidine tag at its carboxyl-terminus. At slightly acidic environment, the histidine-tagged YidC protein efficiently formed a complex with ribosome, irrespective on the translation state, while the interaction was strongly inhibited at physiological pH or upon removal of the tag. In contrast, membrane-reconstituted YidC was competent for binding translating ribosomes at the physiological pH, thus highlighting the importance of a relevant molecular environment. The lack of an interaction between YidC and non-programmed ribosomes points at a critical role of the emerging nascent chain in targeting of the RNCs to the membrane insertase. In agreement with our findings, Welte *et al.* have recently reported weak and surface-scattered interactions between non-translating ribosomes and YidC incorporated in native membranes, which could only be detected by mass spectroscopy analysis upon chemical cross-linking [15]. Future studies should address the specificity of YidC to nascent chains of different lengths and hydrophobicity in order to reveal the determinants of the insertion pathway [24,36].

Interestingly, a recent effort on studying interaction partners for YidC incorporated into nanodiscs did not reveal interactions with ribosomes or any other cytoplasmic macromolecule [37]. In that study, Zhang et al. employed a specific reconstitution procedure in which no additional lipids were supplied that resulted in tight packing of YidC within the nanodisc. Because of spatial considerations, this may have caused interference with the ability of YidC to bind ribosomes, also as our data indicate that the lipid environment is an

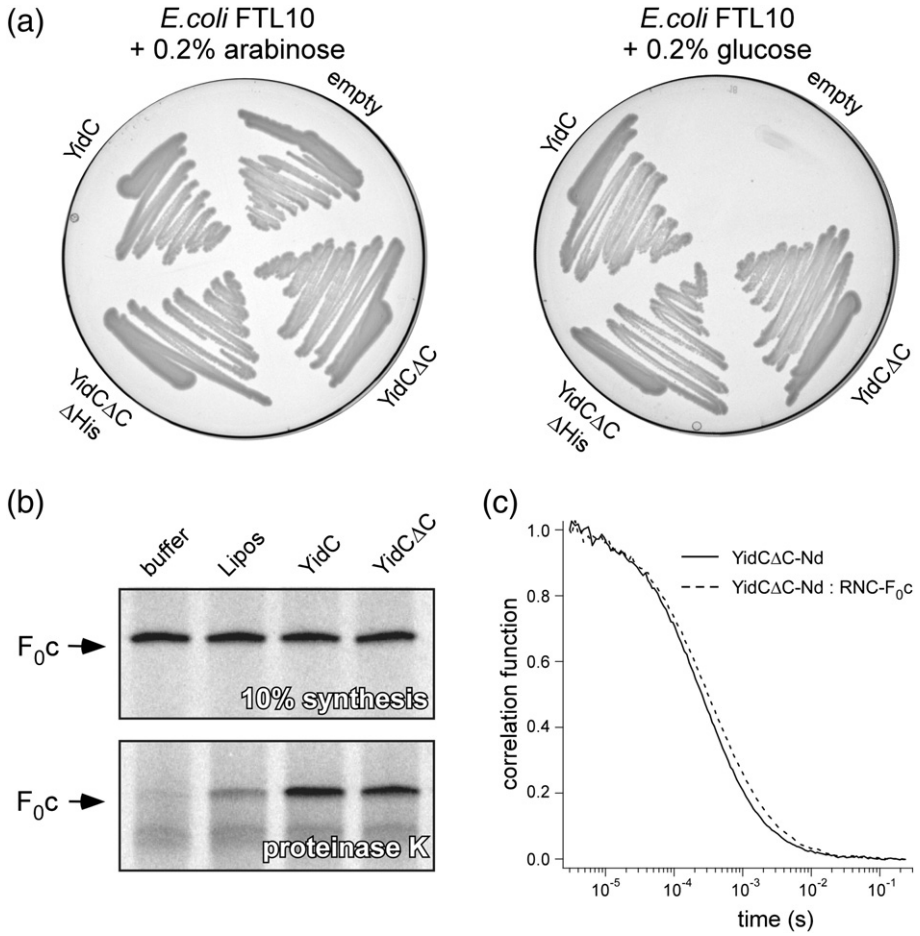

Fig. 5. The C-terminal domain of YidC is not essential for YidC activity. (a) YidC C-terminal deletion does not affect bacterial growth. Truncated forms of YidC that lack the C-terminal domain ("YidCΔC") and the hexa-histidine tag ("YidCΔCΔHis") supported the bacterial viability at the endogenous YidC-depleting conditions in the absence of arabinose. Cells transformed with either an empty pTrc99a vector ("empty") or a plasmid encoding for wild-type YidC ("YidC") were used as a negative and positive controls, respectively. (b) YidC C-terminus is not essential for activity *in vitro*. Both wild-type YidC and YidCΔC supported insertion of F_0c substrate protein into proteoliposomes. (c) The YidC:RNC interaction is stimulated by the C-terminal domain of YidC. Normalized auto-correlation curves recorded on histidine-tagged YidCΔC-Nd in the absence and presence of 300 nM RNCs at pH 7.5 are shown. The shift in the FCS curves describes ribosome binding to 21 ± 3% YidC.

essential component for the YidC:ribosome complex assembly, suggesting that the native interactions were abolished in the lipid-free reconstituted system.

The Oxa1 insertase contains a long (>150 amino acids) and positively charged C-terminal domain that was demonstrated to bind ribosomes. Driven by strong electrostatic interactions, the Oxa1:ribosome binding also occurs in the absence of the emerging nascent chain [27], and the isolated C-terminal domain was shown to interact strongly with ribosomes [26,38]. Though being a likely evolutionary ancestor for eukaryotic insertases [39], YidC proteins of Gram-negative bacteria differ from Oxa1 in their C-termini. This region of the *E. coli* YidC contains only 13 amino acids, with a net charge of +7 [29], and is not essential for activity as the truncated variant YidCΔC fully complements the insertase functioning *in vivo*, in agreement with previous studies [14]. We now show that the YidC:RNC binding and the insertase activity of reconstituted YidC are not completely abolished upon removal of the YidC C-terminal domain, explaining its functional properties. Being present in abundance within the bacterial membrane [40], YidC may support protein insertion even if the affinity to the ribosome is reduced by the C-terminal domain deletion. This suggests that other docking sites on YidC contribute to ribosome binding. A possible candidate is the cytoplasmic loop L2 that contains approximately 50 amino acid residues with a net charge of +11 [29].

With limited insight into the structure of YidC, its functional oligomeric state is not well established,

though it might be a crucial factor for the insertase functioning. Initially, dimers of overexpressed YidC were observed by blue-native PAGE [22] and membrane-reconstituted YidC was shown to form dimers upon tight packing within two-dimensional crystals, though no contact points between the protomers were observed in the density maps [17]. The latest cryo-EM efforts visualized a feature-less density at the ribosomal tunnel exit that was assigned to a YidC dimer based on its spatial dimensions [16]. Furthermore, the YidC homologues Alb3 and Oxa1 were suggested to form dimers or tetramers [41,42], which may be arranged to form a consolidated pore of 1–2 nm diameter within the membrane [43]. Here, we employed a quantitative FCCS approach to characterize the quaternary state of YidC while bound to the ribosome. Our experiments did not reveal YidC oligomers upon purification, suggesting either that YidC is present as monomers or that the interactions between the protomers are weak or transient in agreement with the loose packing of YidC protomers within two-dimensional crystals [17]. In contrast to the previous structural model for the YidC:ribosome complex, we demonstrated here for the first time that monomeric YidC is sufficient to bind a translating ribosome, both in the detergent-solubilized state and at the lipid membrane interface, although oligomers of YidC bound to RNCs at specific conditions (low pH, excess of YidC). Importantly, multiple copies of YidC reconstituted within a nanodisc did not stimulate the interaction with ribosomes; thus, the YidC:ribosome complex involves binding sites within a single YidC molecule. However, as YidC:ribosome binding at the membrane interface represents an initial step during YidC-driven substrate insertion, further YidC oligomerization via intramembrane protein:protein interactions along the functional cycle cannot be excluded and will be examined in future studies.

Experimental Procedures

YidC cloning

A C-terminal hexa-histidine tag and a double factor Xa protease cleavage site (IEGR) were introduced into the wild-type YidC by overlap PCR. The resulting gene encoding for $YidC^{FX}$ protein was ligated into pTrc99a vector [44] using XbaI and HindIII restriction sites and transformed into DH5α cells [45]. An endogenous cysteine residue at position 423 within YidC was exchanged for a serine by QuikChange mutagenesis, and a unique cysteine was introduced at position 269 replacing an aspartate within a solvent-exposed region of the large periplasmic domain P1 based on its crystal structure [20] resulting in a plasmid pKA107. The sequence encoding the factor Xa site was further removed by PCR and a following blunt-end ligation (plasmid pKA109), and a YidC variant lacking 13 amino acids at its C-terminal end (YidCΔC) and the histidine tag (YidCΔCΔHis) was prepared in an analogous way (plasmids pKA131 and pKA132, respectively). All cloning steps were verified by sequence analysis (Macrogen Europe).

In vivo complementation assay

To study functional properties of YidCΔC *in vivo*, we transformed *E. coli* FTL10 strain cells [35] either with the plasmid pKA107, pKA131, and pKA132 or with the empty pTrc99a vector. After initial growth in the presence of arabinose, the cells were grown out on LB-agar plates containing either 0.2% arabinose or 0.2% glucose. Growing FTL10 strain in the absence of arabinose does not allow for endogenous YidC expression; thus, the effect of YidC depletion can be inferred from the colony phenotype.

YidC purification

Histidine-tagged YidC variants were overexpressed in *E. coli* SF100 strain [46] as described before [22], and YidC was purified from total membrane vesicles by Ni^{+}-NTA chromatography. Hereto, membrane vesicles were solubilized by 2% DDM in the presence of 100 mM potassium phosphate (pH 7.5), 100 mM KCl, 10% glycerol, and 200 μM tris(2-carboxyethyl)phosphine to prevent disulfide bond formation. The protein was bound to Ni^{+}-NTA agarose (Qiagen) and washed with a buffer containing 50 mM imidazole (Roth). Ni^{+}-NTA-bound YidC was incubated with maleimide derivatives of AlexaFluor 488 or Atto 647N at pH 7.0–7.3 to maximize specific labeling of cysteine residues. YidC was eluted with a buffer containing 400 mM imidazole, and the protein yield and the labeling efficiency were determined spectrophotometrically. The extinction coefficients used were: ε_{280} = 96,000 cm^{-1} M^{-1} for YidC, ε_{500} = 72,000 cm^{-1} M^{-1} for AlexaFluor 488, and ε_{640} = 150,000 cm^{-1} M^{-1} for Atto 647N. The labeling efficiency typically ranged between 90% and 110% for each fluorophore, and unspecific labeling did not exceed 10% as assayed on cysteine-less YidC. To validate the activity of YidC, we reconstituted the protein either in *E. coli* polar lipid extract or synthetic liposomes composed of 30% 1,2-dioleoyl-*sn*-glycero-3-phospho-(1′-rac-glycerol), 30% 1,2-dioleoyl-*sn*-glycero-3-phosphoethanolamine, and 40% 1,2-dioleoyl-*sn*-glycero-3-phosphocholine (Avanti Polar Lipids), without diacylglycerol supplements. Synthetic liposomes were prepared as previously described [21]. Activity was tested by measuring the YidC-dependent insertion of F_0c subunit of F_1F_0 ATP synthase as described previously [22].

Cleavable hexa-histidine tag was removed from YidC^{FX} by incubating the protein in the detergent solution with 100-fold diluted factor Xa protease (Sigma-Aldrich) at 25 °C for 3 h. A control YidC^{FX} sample was incubated in the absence of the protease. In the protease-treated sample, the minor levels of non-processed YidC were removed using Ni^{+}-NTA-conjugated agarose (Qiagen). Tag removal was confirmed by SDS-PAGE and following Western blotting against the histidine tag. Unspecific degradation upon the treatment was within 15% of the total YidC amount as judged from SDS-PAGE.

Nanodisc reconstitution of YidC

To analyze the YidC:RNC interaction in a lipid environment, we reconstituted histidine-tagged YidC into small lipid patches known as nanodiscs [33] according to the method used for the SecYEG complex [24] with minor modifications. MSP1D1 scaffold protein (MSP) was used to form nanodiscs of ≈10 nm diameter, and the reconstitution reaction was carried out in the presence of the synthetic lipid mixture described above. YidC:MSP:lipid ratios were 1:10:250 and 10:10:250 to obtain YidC^{mono}-Nd and YidC^{oligo}-Nd samples, respectively. Detergents were removed by Bio-Beads SM2 sorbent (Bio-Rad), and the reconstituted samples were centrifuged at 250,000 *g* for 30 min to remove minute amounts of formed proteoliposomes. Size-exclusion chromatography was performed by fast protein liquid chromatography using a Superdex 10/300 Tricorn column (GE Healthcare), and 1-mL elution fractions were collected in 50 mM Tris–HCl (pH 7.5), 100 mM KCl, and 5% glycerol (buffer N). To ensure the equality of nanodiscs for YidC^{mono}-Nd and YidC^{oligo}-Nd, we prepared samples in parallel and corresponding #14 fractions of the size-exclusion chromatography were used in the experiments.

Ribosome isolation

Non-programmed ribosomes were prepared as previously described [24]. To derive stable ribosomes charged with F_0c nascent chains (RNC-F_0c), we exchanged the PstI-EcoRV fragment of the plasmid pUC19Strep$_3$FtsQSecM [47] with a fragment coding for the first 44 residues of *E. coli* F_0c that include the first transmembrane domain and a fragment of the cytoplasmic loop. The resulting translation product contained an N-terminal triple Strept tag and was followed by a SecM stalling sequence with a total length of 123 amino acids. While the SecM polypeptide occupies the ribosomal tunnel, the first transmembrane domain of F_0c becomes exposed at the tunnel exit at the stalled ribosomes, thus mimicking a translation intermediate. The designed plasmid (pJK763) was verified by sequence analysis (Macrogen Europe). RNC-F_0c were expressed and purified by sedimentation followed by a StrepTactin column (IBA) chromatography as previously described [24].

Fluorescence correlation spectroscopy

Detergent-solubilized YidC labeled with AlexaFluor 488 and Atto 647N was diluted 50-fold into 100 mM KCl, 10 mM $MgCl_2$, 5% glycerol, 0.1% DDM, and 25 mM ADA buffer (pH 6.2 or pH 7.4) (buffers A and P, respectively) prior to fluorescence measurements. To remove aggregates, we centrifuged the samples at 350,000 *g* for 30 min. If necessary, samples were further diluted to achieve YidC concentration of 50–100 nM as required for the FCS analysis [23]. Nanodisc-reconstituted YidC was analyzed in buffer N supplemented with 10 mM $MgCl_2$ and the YidC-Nd concentration was adjusted for needs of FCS.

FCS/FCCS experiments were performed on an LSM 710 inverted confocal microscope (Zeiss GmbH) equipped with a ConfoCor 3 unit. YidC-conjugated fluorophores were excited by a He-Ne laser at 488 nm and an argon laser at 633 nm. Emitted light was split on a dichroic mirror and collected in two channels of 505–610 nm (AlexaFluor 488 emission) and 655–710 nm (Atto 647N emission). Diffusion of free AlexaFluor 488 and AlexaFluor 633 in water was monitored to determine the waist radii (ω_0) for the laser excitation volumes (180 nm and 240 nm, respectively) and to control the cross-talk level in FCCS [48]. The structure parameter defined as the ratio between the axial and waist radii of the excitation volume (z_0/ω_0) was 5. Diffusion analysis on YidC and YidC:ribosome complexes was performed as described previously [24].

As a reference for FCCS recordings, the fluorophores were conjugated to a double-stranded DNA and the cross-correlation signal was measured on the DNA diffusion in water. The experimental cross-correlation signal ranged between 80% and 90% of theoretically calculated maximum level. FCCS signal measured for diffusion of YidC-AlexaFluor 488 and YidC-Atto 647N was used to detect YidC oligomers within the studied samples, and only YidC dimers described in previous studies were considered. The ratio between autocorrelation and cross-correlation signal amplitudes was used to quantify the concentration of dual-labeled YidC dimers as previously described [48]. FCCS does not detect YidC oligomers bearing fluorophores of the same type; thus, this fraction of dimers was calculated based on FCS-derived YidC concentrations and assuming that YidC oligomerization was stochastic and did not depend on the fluorophore type.

FRET measurements

Histidine-tagged YidC proteins labeled with AlexaFluor 488 and Cy3 dyes were mixed at 1:1 molar ratio and diluted to a final concentration of 100 nM in buffer A. Indicated amounts of RNC-F_0c were added and

incubated 10 min at room temperature. FRET experiments were performed on SLM2 Aminco Baumann spectrophotometer. Donor fluorophore AlexaFluor 488 was excited at 480 nm, and emission spectra of donor and acceptor dyes were recorded between 500 and 650 nm. The fluorescence was normalized for the signal intensity of free YidC at 520 nm.

Acknowledgements

We would like to thank Dr. M. J. Saller for many valuable comments and discussions on the project and Dr. N. Dudkina and Prof. E. J. Boekema for negative-stain electron microscopy experiments. This work was supported by the Chemical Sciences division of the Netherlands Foundation for Scientific Research. M.S. was supported by the International Erasmus Programme.

Conflict of Interest: The authors declare no conflict of interests.

Appendix A. Supplementary data

Supplementary data to this article can be found online at http://dx.doi.org/10.1016/j.jmb.2013.07.042.

Received 13 May 2013;
Received in revised form 24 June 2013;
Accepted 9 July 2013
Available online 8 August 2013

Keywords:
macromolecular assembly;
membrane protein;
membrane insertase;
single-molecule biophysics;
ribosome

Present address: M. Sustarsic, Clarendon Laboratory, Department of Physics, University of Oxford, Oxford OX1 3PU, United Kingdom.

Abbreviations used:
DDM, *n*-dodecyl β-D-maltoside; cryo-EM, cryo-electron microscopy; FCS, fluorescence correlation spectroscopy; FCCS, fluorescence cross-correlation spectroscopy; FRET, Förster resonance energy transfer; MSP, major scaffold protein; RNC, ribosome:nascent chain.

References

[1] Fiedler S, Broecker J, Keller S. Protein folding in membranes. Cell Mol Life Sci 2010;67:1779–98.
[2] du Plessis DJ, Nouwen N, Driessen AJ. The Sec translocase. Biochim Biophys Acta 2011;1808:851–65.
[3] Luirink J, Yu Z, Wagner S, de Gier JW. Biogenesis of inner membrane proteins in *Escherichia coli*. Biochim Biophys Acta 2012;1817:965–76.
[4] Wang P, Dalbey RE. Inserting membrane proteins: the YidC/Oxa1/Alb3 machinery in bacteria, mitochondria, and chloroplasts. Biochim Biophys Acta 2011;1808:866–75.
[5] van der Laan M, Bechtluft P, Kol S, Nouwen N, Driessen AJ. F1F0 ATP synthase subunit c is a substrate of the novel YidC pathway for membrane protein biogenesis. J Cell Biol 2004;165:213–22.
[6] Samuelson JC, Chen M, Jiang F, Moller I, Wiedmann M, Kuhn A, et al. YidC mediates membrane protein insertion in bacteria. Nature 2000;406:637–41.
[7] Serek J, Bauer-Manz G, Struhalla G, van den Berg L, Kiefer D, Dalbey R, et al. *Escherichia coli* YidC is a membrane insertase for Sec-independent proteins. EMBO J 2004;23:294–301.
[8] Winterfeld S, Ernst S, Borsch M, Gerken U, Kuhn A. Real time observation of single membrane protein insertion events by the *Escherichia coli* insertase YidC. PLoS One 2013;8:e59023.
[9] Gray AN, Henderson-Frost JM, Boyd D, Sharafi S, Niki H, Goldberg MB. Unbalanced charge distribution as a determinant for dependence of a subset of *Escherichia coli* membrane proteins on the membrane insertase YidC. MBio 2011;2. doi:10.1128/mBio.00238-11.
[10] Kol S, Majczak W, Heerlien R, van der Berg JP, Nouwen N, Driessen AJ. Subunit a of the F(1)F(0) ATP synthase requires YidC and SecYEG for membrane insertion. J Mol Biol 2009;390:893–901.
[11] Price CE, Driessen AJ. Conserved negative charges in the transmembrane segments of subunit K of the NADH:ubiquinone oxidoreductase determine its dependence on YidC for membrane insertion. J Biol Chem 2010;285:3575–81.
[12] Nagamori S, Smirnova IN, Kaback HR. Role of YidC in folding of polytopic membrane proteins. J Cell Biol 2004;165:53–62.
[13] Wagner S, Pop OI, Haan GJ, Baars L, Koningstein G, Klepsch MM, et al. Biogenesis of MalF and the MalFGK(2) maltose transport complex in *Escherichia coli* requires YidC. J Biol Chem 2008;283:17881–90.
[14] Jiang F, Chen M, Yi L, de Gier JW, Kuhn A, Dalbey RE. Defining the regions of *Escherichia coli* YidC that contribute to activity. J Biol Chem 2003;278:48965–72.
[15] Welte T, Kudva R, Kuhn P, Sturm L, Braig D, Muller M, et al. Promiscuous targeting of polytopic membrane proteins to SecYEG or YidC by the *Escherichia coli* signal recognition particle. Mol Biol Cell 2012;23:464–79.
[16] Kohler R, Boehringer D, Greber B, Bingel-Erlenmeyer R, Collinson I, Schaffitzel C, et al. YidC and Oxa1 form dimeric insertion pores on the translating ribosome. Mol Cell 2009;34:344–53.
[17] Lotz M, Haase W, Kuhlbrandt W, Collinson I. Projection structure of yidC: a conserved mediator of membrane protein assembly. J Mol Biol 2008;375:901–7.
[18] Boy D, Koch HG. Visualization of distinct entities of the SecYEG translocon during translocation and integration of bacterial proteins. Mol Biol Cell 2009;20:1804–15.
[19] Cross TA, Sharma M, Yi M, Zhou HX. Influence of solubilizing environments on membrane protein structures. Trends Biochem Sci 2011;36:117–25.

[20] Ravaud S, Stjepanovic G, Wild K, Sinning I. The crystal structure of the periplasmic domain of the *Escherichia coli* membrane protein insertase YidC contains a substrate binding cleft. J Biol Chem 2008;283:9350–8.
[21] Kedrov A, Kusters I, Krasnikov VV, Driessen AJ. A single copy of SecYEG is sufficient for preprotein translocation. EMBO J 2011;30:4387–97.
[22] van der Laan M, Houben EN, Nouwen N, Luirink J, Driessen AJ. Reconstitution of Sec-dependent membrane protein insertion: nascent FtsQ interacts with YidC in a SecYEG-dependent manner. EMBO Rep 2001;2:519–23.
[23] Krichevsky O, Bonnet G. Fluorescence correlation spectroscopy: the technique and its applications. Rep Prog Phys 2002;65:251–97.
[24] Wu ZC, de Keyzer J, Kedrov A, Driessen AJ. Competitive binding of the SecA ATPase and ribosomes to the SecYEG translocon. J Biol Chem 2012;287:7885–95.
[25] Kunji ER, Harding M, Butler PJ, Akamine P. Determination of the molecular mass and dimensions of membrane proteins by size exclusion chromatography. Methods 2008;46: 62–72.
[26] Haque ME, Elmore KB, Tripathy A, Koc H, Koc EC, Spremulli LL. Properties of the C-terminal tail of human mitochondrial inner membrane protein Oxa1L and its interactions with mammalian mitochondrial ribosomes. J Biol Chem 2010;285:28353–62.
[27] Jia L, Dienhart M, Schramp M, McCauley M, Hell K, Stuart RA. Yeast Oxa1 interacts with mitochondrial ribosomes: the importance of the C-terminal region of Oxa1. EMBO J 2003;22:6438–47.
[28] Palmer SR, Crowley PJ, Oli MW, Ruelf MA, Michalek SM, Brady LJ. YidC1 and YidC2 are functionally distinct proteins involved in protein secretion, biofilm formation and cariogenicity of *Streptococcus mutans*. Microbiology 2012;158:1702–12.
[29] Saaf A, Monne M, de Gier JW, von Heijne G. Membrane topology of the 60-kDa Oxa1p homologue from *Escherichia coli*. J Biol Chem 1998;273:30415–8.
[30] Heuberger EH, Veenhoff LM, Duurkens RH, Friesen RH, Poolman B. Oligomeric state of membrane transport proteins analyzed with blue native electrophoresis and analytical ultracentrifugation. J Mol Biol 2002;317:591–600.
[31] Schwille P, Meyer-Almes FJ, Rigler R. Dual-color fluorescence cross-correlation spectroscopy for multicomponent diffusional analysis in solution. Biophys J 1997;72: 1878–86.
[32] Seddon AM, Curnow P, Booth PJ. Membrane proteins, lipids and detergents: not just a soap opera. Biochim Biophys Acta 2004;1666:105–17.
[33] Denisov IG, Grinkova YV, Lazarides AA, Sligar SG. Directed self-assembly of monodisperse phospholipid bilayer nanodiscs with controlled size. J Am Chem Soc 2004;126:3477–87.
[34] Ritchie TK, Grinkova YV, Bayburt TH, Denisov IG, Zolnerciks JK, Atkins WM, et al. Chapter 11—reconstitution of membrane proteins in phospholipid bilayer nanodiscs. Methods Enzymol 2009;464:211–31.
[35] Hatzixanthis K, Palmer T, Sargent F. A subset of bacterial inner membrane proteins integrated by the twin-arginine translocase. Mol Microbiol 2003;49:1377–90.
[36] Zhu L, Wasey A, White SH, Dalbey RE. Charge composition features of model single-span membrane proteins that determine selection of YidC and SecYEG translocase pathways in *Escherichia coli*. J Biol Chem 2013;288:7704–16.
[37] Zhang XX, Chan CS, Bao H, Fang Y, Foster LJ, Duong F. Nanodiscs and SILAC-based mass spectrometry to identify a membrane protein interactome. J Proteome Res 2012;11: 1454–9.
[38] Haque ME, Spremulli LL, Fecko CJ. Identification of protein–protein and protein–ribosome interacting regions of the C-terminal tail of human mitochondrial inner membrane protein Oxa1L. J Biol Chem 2010;285:34991–8.
[39] Funes S, Kauff F, van der Sluis EO, Ott M, Herrmann JM. Evolution of YidC/Oxa1/Alb3 insertases: three independent gene duplications followed by functional specialization in bacteria, mitochondria and chloroplasts. Biol Chem 2011;392:13–9.
[40] Urbanus ML, Froderberg L, Drew D, Bjork P, de Gier JW, Brunner J, et al. Targeting, insertion, and localization of *Escherichia coli* YidC. J Biol Chem 2002;277:12718–23.
[41] Nargang FE, Preuss M, Neupert W, Herrmann JM. The Oxa1 protein forms a homooligomeric complex and is an essential part of the mitochondrial export translocase in *Neurospora crassa*. J Biol Chem 2002;277:12846–53.
[42] Dunschede B, Bals T, Funke S, Schunemann D. Interaction studies between the chloroplast signal recognition particle subunit cpSRP43 and the full-length translocase Alb3 reveal a membrane-embedded binding region in Alb3 protein. J Biol Chem 2011;286:35187–95.
[43] Kruger V, Deckers M, Hildenbeutel M, van der Laan M, Hellmers M, Dreker C, et al. The mitochondrial oxidase assembly protein1 (Oxa1) insertase forms a membrane pore in lipid bilayers. J Biol Chem 2012;287:33314–26.
[44] Amann E, Ochs B, Abel KJ. Tightly regulated tac promoter vectors useful for the expression of unfused and fused proteins in *Escherichia coli*. Gene 1988;69:301–15.
[45] Hanahan D. Studies on transformation of *Escherichia coli* with plasmids. J Mol Biol 1983;166:557–80.
[46] Baneyx F, Georgiou G. *In vivo* degradation of secreted fusion proteins by the *Escherichia coli* outer membrane protease OmpT. J Bacteriol 1990;172:491–4.
[47] Schaffitzel C, Ban N. Generation of ribosome nascent chain complexes for structural and functional studies. J Struct Biol 2007;158:463–71.
[48] Bacia K, Schwille P. Practical guidelines for dual-color fluorescence cross-correlation spectroscopy. Nat Protoc 2007;2:2842–56.